Moderate Resolution Imaging Spectroradiometer (MODIS) Cloud Fraction Technical Document

1. Intent of This Document

This document is intended for users who wish to compare satellite-derived observations with climate model output in the context of the CMIP5/IPCC experiments. It summarizes essential information needed for comparing this dataset to climate model output. References and useful links are provided.

This dataset is provided as part of an effort to increase the usability of NASA satellite observational data for the modeling and model analysis communities. In this case, it is equivalent to a standard satellite instrument product (not reprocessed, reformatted, or created solely for comparisons with climate model output). Feedback to improve and validate the dataset for modeling usage is appreciated. Email comments to HQ-CLIMATE-OBS@mail.nasa.gov.

Dataset Filename:

clt_MODIS_L3_C5_200003-201109.nc

Ancillary Filenames:

cltNobs_MODIS_L3_C5_200003-201109.nc,
cltStddev_MODIS_L3_C5_200003-201109.nc

Technical Point of Contact:

Steven A. Ackerman, University of Wisconsin–Madison, stevea@ssec.wisc.edu
Steven Platnick, NASA Goddard Space Flight Center, steven.platnick@nasa.gov

2. Data Origin and Field Description

MODIS (Moderate Resolution Imaging Spectroradiometer) is a key instrument aboard the Terra and Aqua satellites (launched in December 1999 and May 2002, respectively). Both satellites are in a sun-synchronous orbit. Terra's orbit is timed so that daytime descending passes (from north to south) cross the equator in the morning (1030 LT), while Aqua ascending passes (south to north) occur over the equator in the afternoon (1330 LT). These orbits, with a 16-day repeat cycle on the World Reference System (WRS-2) grid, are precisely controlled and have remained extremely stable in both space and time. With a 2330 km swath, each MODIS instrument views the entire Earth's surface every 1 to 2 days, acquiring data in 36 spectral channels (or “bands” in MODIS nomenclature). See Section 6 for an overview of the MODIS instrument.

The pixel-level (Level-2) MODIS cloud mask (archived product filename MOD35 and MYD35 for MODIS Terra and Aqua, respectively) is at a native spatial resolution of 1km. The cloud mask algorithm is identical for both instruments. Results from this mask are aggregated to a global 1° gridded (Level-3) cloud fraction with daily, eight-day, and monthly temporal

resolution. The monthly aggregation is contained within archived product names MOD08_M3 and MYD08_M3, respectively.

For CMIP5, monthly cloud fraction (averaged from daytime and nighttime orbits) is provided only for MODIS Terra and covers the time period from March 2000 through a recently available processed month (September 2011 at the time of this writing). The product contains temporal and geometric fields (time, latitude, and longitude) along with the mean cloud fraction. The time corresponds to the first day of the month and is given as the number of days since March 1, 2000. The latitude and longitude grid is equal-angle at 1° resolution. The longitude grid center range is from 0.5 to 359.5 degrees while the latitude extends from -89.5 to +89.5 degrees (south to north). The value of cloud fraction is given in percent (i.e., minimum and maximum values of 0 and 100) and is equivalent to values provided by the Science Data Set name "Cloud_Fraction_Mean_Mean" in the archived MOD08_M3 Hierarchical Data Format (HDF) file available through the Level-1 and Atmosphere Archive and Data Distribution System (LAADS) at NASA Goddard Space Flight Center.

CF variable name, units	Long_Name: Total Cloud Fraction Standard Name: cloud_area_fraction units: dimensionless (percent)
Spatial resolution	1° equal angle
Temporal resolution and extent	Monthly average, from March 2000–September 2011
Coverage	Global

The dataset includes two ancillary files. File named *cltStddev_MODIS_L3_C5_200003-201109.nc* provides the standard deviation of the individual daily cloud fractions that comprise the month, for each equal-angle 1° grid. It is derived from the MODIS cloud mask (MOD35) and identical to MODIS Level-3 monthly (MOD08_M3) SDS name *Cloud_Fraction_Mean_Std*. File named *cltNobs_MODIS_L3_C5_200003-201109.nc* gives the total monthly counts for all cloudy pixels, for each 1° grid. It is derived from the MODIS cloud mask (MOD35) and identical to MODIS Level-3 monthly (MOD08_M3) SDS name *Cloud_Fraction_Pixel_Counts*. There are data points having zero standard deviations. They correspond to observing clear sky scenes (0%) or fully cloudy scenes (99.99% or 100%) for a whole month, over which the standard deviations are smaller than the fixed precision 1e-4 used in the data set.

3. Data Product Algorithm Overview

MODIS measures radiances in 36 spectral bands from the visible to the infrared with spatial resolution from 250 m to 1 km. The monthly cloud fraction in the CMIP5 data set is derived from the Level-2 MODIS cloud mask (MOD35). The details of the cloud mask algorithm may be found in Ackerman et al., (1998), King et al., (2003), Platnick et al., (2003), Ackerman et al., (2010) and Frey et al., (2008).

Cloud detection is based on the contrast (i.e., cloud vs. background surface) for a given target area. Contrast may be defined as differing signals for individual spectral bands (e.g. clouds are generally more reflective in the visible but colder than the background as measured in the thermal IR), spectral combinations (e.g. 0.86/0.66 μm ratio is close to unity for cloudy skies), or temporal and spatial variations of these. The MODIS cloud mask uses several cloud detection tests to indicate a level of confidence that MODIS is observing a clear sky scene. Produced for the entire globe, day and night, and at 1-km resolution, the cloud mask algorithm employs up to

twenty-two MODIS spectral bands (250-m and 500-m band radiances aggregated to 1-km) to maximize reliable cloud detection. In addition, a 250-m mask derived from the two 250 m resolution bands (0.65 and 0.86 μm) in combination with 1-km cloud mask results is produced and archived, but will not be discussed here. The 1-km mask is independent of the 250-m mask. The cloud mask assesses the likelihood that clouds obstruct a given pixel. As cloud cover can occupy a pixel to varying extents, the MODIS cloud mask is designed to allow for varying degrees of clear sky confidence; the mask summarizes its result from all individual tests by classifying cloud contamination in every pixel of data as either confident clear, probably clear, uncertain/probably cloudy, or cloudy.

The MODIS cloud mask algorithm identifies several domains according to surface type and solar illumination including land, water, snow/ice, desert, and coast for both day and night. Once a pixel is assigned to a particular domain (defining an algorithm path), a series of threshold tests attempts to detect the presence of clouds or optically thick aerosol in the instrument field-of-view. Each test returns a confidence level that the pixel is clear ranging in value from 1 (high confidence clear) to 0 (very low confidence clear or high confidence of cloud or other obstruction). Ackerman et al. (1998) provides details of confidence calculations for individual spectral tests. There are several types of tests, where detection of various cloud conditions relies on different sets of spectral measures. Those capable of detecting similar cloud conditions are grouped together. While these groups are arranged so that independence between them is maximized; few, if any, spectral tests are completely independent. As described by Ackerman et al. (1998), a minimum confidence is determined for each group as follows:

$$G_{j=1\text{-}N} = \min[F(i,j)]_{i=1\text{-}m}$$

where $F(i,j)$ is the confidence level of an individual spectral test, m is the number of tests in a given group, j is the group index, and N is the number of groups (*e.g*. 5). The final cloud mask confidence (Q) is then determined from the products of the results for each group,

$$Q = \sqrt[N]{\prod_{i=1}^{N} G_j}$$

The four confidence levels included in the cloud mask output are: (1) confident clear (Q > 0.99); (2) probably clear (Q > 0.95); (3) uncertain/probably cloudy (Q > 0.66); and (4) cloudy (Q ≤ 0.66). These outcomes constitute bits 1 and 2 of the mask. Note that the result gives the confidence, or lack thereof, in the existence of a clear pixel and not the confidence in the presence of an overcast cloudy pixel. As such, the cloudy outcome can alternately be labeled as not clear (i.e., high confidence in an obstruction in the field of view).

This approach is clear-sky conservative in the sense that if any test is highly confident that a scene is cloudy (Fi,j = 0), the final clear sky confidence is also 0. However, it is also the case that the overall mask cannot be clear-sky conservative if individual test thresholds are set to flag only thick cloud or overcast conditions. Therefore, thresholds are set so that they detect the maximum number of cloudy pixels without generating unacceptably large number of "false alarms" (clear pixels incorrectly flagged as cloudy). An attempt has been made to represent regional and global cloud fractions by aggregating pixels flagged as either cloudy or probably cloudy. Detailed information is contained in Ackerman et al., (1998), Frey et al., (2008), and Ackerman et al., (2008).

4. Validation and Uncertainty Estimates

MODIS cloud mask results have been validated against a variety of observations (other satellite retrievals, lidars and radars). This section summarizes the results of a comparison of MODIS cloud detection with collocated CALIOP Cloud-Aerosol Lidar with Orthogonal Polarization) classifications of the scene (Holz et al., 2008) and sensitivity studies presented in Ackerman et al. 2008.

Global results of cloud mask comparisons against the 1-km CALIOP cloud products for August 2006 and February 2007 were presented by Holz et al. (2009) (see Table 1). For the comparison, a MODIS cloud mask result was considered cloudy if the cloud mask returned confident cloud or probably cloudy, while a MODIS pixel is determined clear if the MODIS cloud mask returns probably clear or confidently clear. Only MODIS pixels where all the collocated CALIOP retrievals are identical (i.e., either all clear or all cloudy) are included in the statistics in Table 1. Results are separated by clear and cloudy FOV as determined by CALIOP, as well as categorized by day and night, surface type, polar and non-polar regions.

The global agreement between MODIS and CALIOP 1-km layer products in identifying clear scenes is greater than 84%, which is in general agreement with previous results (Ackerman et al., 2008). For both daytime and nighttime cloud detection the MODIS cloud mask is in closer

Table 1: The global fractional agreement of cloud detection between MODIS and CALIPSO lidar (CALIOP) for August 2006 and February 2007. The results are separated by CALIOP averaging amount, with the 5 km averaging results in parenthesis, as well as day, night and surface type. (Holz et al 2008)

	August 2006 Clear	August 2006 Cloudy	February 2006 Clear	February 2006 Cloudy
Global Day/Night CALIOP 1-km	0.84	0.88	0.85	0.88
Non-Polar Day/Night CALIOP 1-km	0.87	0.91	0.85	0.90
Non-Polar Day CALIOP 1-km	0.89	0.90	0.87	0.91
Non-Polar Night CALIOP 1-km	0.85	0.91	0.84	0.90
Non-Polar Land CALIOP 1-km	0.90	0.84	0.82	0.85
Non-Polar Ocean CALIOP 1-km	0.86	0.93	0.86	0.93
Arctic > 60° Latitude	0.74	0.90	0.82	0.73
Antarctic < -60° Latitude	0.77	0.73	0.91	0.88

agreement with CALIOP for cloudy scenes than for clear scenes. This result is expected as the MODIS cloud mask was designed to be clear-sky conservative; that is, if there is uncertainty in the spectral tests, the MODIS cloud mask tends to label the scene as cloudy. When the results are separated by day and night, the daytime clear sky agreement with CALIOP improves by approximately 3-4%. The daytime MODIS cloud mask uses solar reflectance channels and this additional information is expected to improve the MODIS cloud mask sensitivity to low clouds and other cloud types having little thermal contrast with the surface. The agreement between instruments in labeling a non-polar scene as cloudy is approximately 90% and is fairly insensitive to solar illumination. The best agreement for non-polar land occurs in August at 90%, and drops to 82% for February. In August, warmer land surfaces and the reduced amount of surface snow/ice in the northern hemisphere both contribute to the increased contrast between clear and cloudy scenes, resulting in an improved clear scene classification. Compared to land, ocean surfaces exhibit less variation in temperature and albedo, and so the agreement over non-polar oceans is similar for both months.

In Arctic regions, CALIOP and MODIS agree that the scene is clear 74% of the time in August and 82% of the time in February; they agree that the scene is cloudy 90% of the time in August and only 73% in February. This suggests that during the summer months the MODIS cloud mask is biased cloudy while in the winter it is biased clear. For the Antarctic the clear sky agreement is 77% for August and 91% for summer; and for cloudy scenes agreement is 73% in August and 88% in February. The disagreement for cloudy FOVs during the Antarctic winter (August 2006) can be partly attributed to CALIOP sensitivity to polar stratospheric clouds.

The MODIS cloud mask retrieval requires good contrast between clear-sky and cloudy-sky conditions. These conditions are dependent on both surface and atmospheric properties and can have significant regional variation. To investigate the regional performance of the cloud mask, the collocated data was divided into five-degree grid cells with the results presented in Figs. 1 and 2. While CALIOP and MODIS are in good global agreement, there are regional variations. For clear-sky, MODIS disagrees with CALIOP immediately north of the coast of Antarctica. MODIS requires a snow/ice mask in its selection of thresholds. Incorrect scene identification leads to cloud detection errors that likely contribute to the disagreement around the coast of Antarctica. In August, there is also a large difference over the Indian subcontinent that occurs primarily during the day. Increase in vegetation growth after the summer monsoon would tend to increase the contrast between clear and cloudy in the solar bands. However, the agreement is worse rather than better and results from the CALIOP detecting more upper-level clouds.

In February, the disagreement in the mid-latitude regions in and near Siberia is associated with cold, snowy surfaces, causing misclassification. The disagreement is frequent during the daylight hours. Disagreement in clear classification also occurs around regions of high clouds, the Amazon and the maritime convective region near Indonesia.

In general there is very good agreement in the regional classification of cloudy scenes (Fig. 2). The largest differences occur in polar regions during winter when the MODIS retrievals must rely only on thermal methods and over very cold surfaces. Disagreement occurs over the Antarctica highlands, with CALIOP sensitive to optically thin polar stratospheric clouds. The disagreements in labeling a scene as cloudy also occur over the tropical deserts, caused by MODIS missing high thin cirrus and misclassification of aerosols as clouds by either MODIS or CALIOP. While the fraction of disagreement is large, the number of cases is generally small in comparison to other geographic regions.

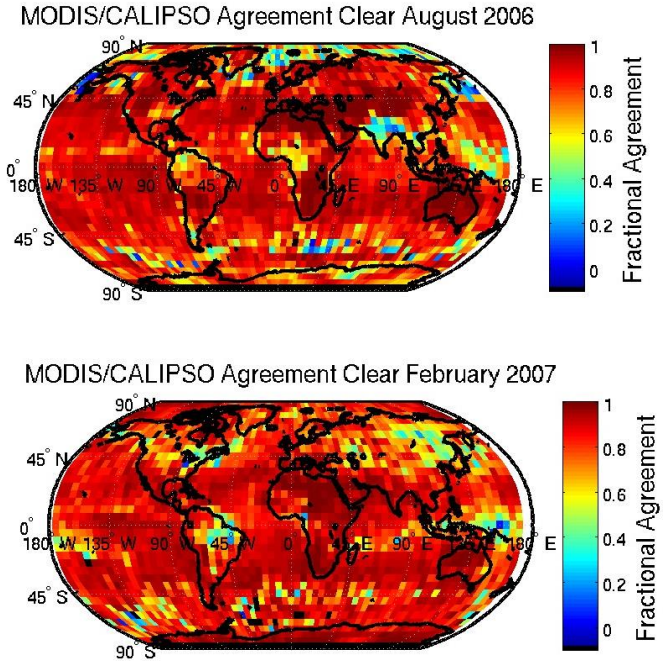

Figure 1. The fractional agreement between the MODIS 1-km and CALIOP 1-km cloud mask for clear scenes. The fractional agreement is calculated at 5-degree resolution in the figure. A grid cell with perfect MODIS agreement will have a fractional agreement of 1 (red) while regions of poorer agreement are colored blue. (Holz et al 2008)

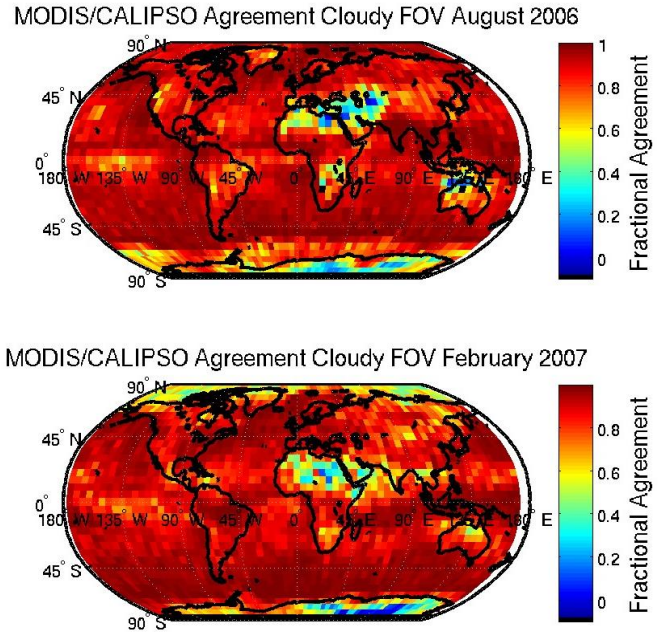

Figure 2. The fractional agreement between the MODIS 1-km and CALIOP 1-km cloud mask for cloudy scenes. The fractional agreement is calculated at 5-degree resolution in the figure. A grid cell with perfect MODIS agreement will have a fractional agreement of 1 (red) while regions of poorer agreement are colored blue. (Holz et al 2008)

Comparisons between MODIS and Arctic High-Spectral Resolution Lidar (AHSRL) show that 80% of clouds are detected by MODIS with optical depths greater than 0.3. This would indicate that only very thin cirrus, with very low ice water paths, will not be detected by MODIS.

5. Consideration for Model-Observation Comparisons

Cloud fraction (or cloud amount) climatologies from existing satellite data records differ in magnitude similar to the MODIS/CALIOP comparison above (e.g. Thomas et al., 2004; Stubenrauch et al., 2009; Stubenrauch et al., 2013). These differences are due to a number of reasons including satellite orbit, spatial resolution and coverage, and instrument detection sensitivity.

More specifically, imager-based estimates depend on the instrument's cloud detection capability (a function of spectral information and instrument performance), spatial resolution (a consequence of partly cloudy pixels) and viewing and illumination geometry. In contrast to spectrally- and/or spatially-challenged heritage imagers, MODIS has 36 spectral bands with at least a 1km spatial resolution at nadir. This combination of spectral and spatial resolutions allow for better detection of cloud types and their associated properties. Regardless, comparisons of model-produced cloud fraction to MODIS estimates will be more robust if they can account for the above sensitivities.

Imager sensitivity is relatively easy to account for. As mentioned at the end of the last section, comparisons of MODIS cloud mask results with co-located lidar observations indicate that cloudy scenes with a total cloud optical extinction of less than about 0.3 are unlikely to be detected as cloudy by the MODIS algorithm (Fig. 15 in Ackerman et al., 2008). More robust comparisons can be made by restricting model estimates of cloud fraction to cloudy columns with optical depth greater than 0.3, perhaps by using a "satellite simulator" (COSP, for example; see Bodas-Salcedo et al., 2011). COSP contains both MODIS and ISCCP simulators, both of which use an optical depth detection threshold of 0.3, so any model that has run the ISCCP simulator already has the detection filtering appropriate for comparing with the MODIS cloud fraction described here. This will have little effect except on models that produce a significant amount of cloudy columns with optical depths equivalent to 0.3 or less.

However, even with a satellite simulator, models cannot characterize the small-scale cloud heterogeneity that gives rise to imager spatial resolution sensitivities (Fig. 7 in Ackerman et al., 2008). Partly cloudy pixels resulting from such heterogeneity are likely responsible for a substantial portion of the optically thin cloud included in MODIS and other imager estimates of cloud fraction (Pincus et al., 2012). Therefore, the ability to usefully compare optically thin columns in models with observations from broken cloud regions is inherently problematic (Pincus et al., 2012; Klein et al., 2012).

Cloud fraction has value for initial model-observation intercomparsions but is fundamentally an ill-posed quantity. As model agreement with cloud fraction improves, comparisons with higher-order cloud products (i.e., infrared-inferred height, optical thickness, particle effective radius, water path) are required to provide important constraints. These comparisons are best made with satellite simulators. A simulator for MODIS is available as part of the COSP package mentioned above and observational data sets matching the output of the simulator are available at http://climserv.ipsl.polytechnique.fr/cfmip-obs/. Comparisons must still account for

observational uncertainties, perhaps by coarse-graining models and observations appropriately (Klein et al., 2012).

This data set is derived from Collection 5 MODIS Level-3 statistics (King et al. 2003; Hubanks 2008; Frey et al. 2008). The cloud fraction, or cloud amount, is obtained from the Level-3 (MOD08) Scientific Data Set (SDS) called 'Cloud_Fraction_Mean_Mean', which is derived from the Level-2 MODIS Cloud Mask (MOD35). This SDS provides the average of the day and nighttime orbit observations from the sun-synchronous satellite. The Cloud Mask returns one of four categories for each 1km pixel: confident cloudy, probably cloudy, probably clear or confident clear. The first two categories are classified as cloudy and the last two as clear in the Level-3 statistics. Using this binary classification may lead to biases in the cloud amount on the order of a few percent (Kotarba 2010).

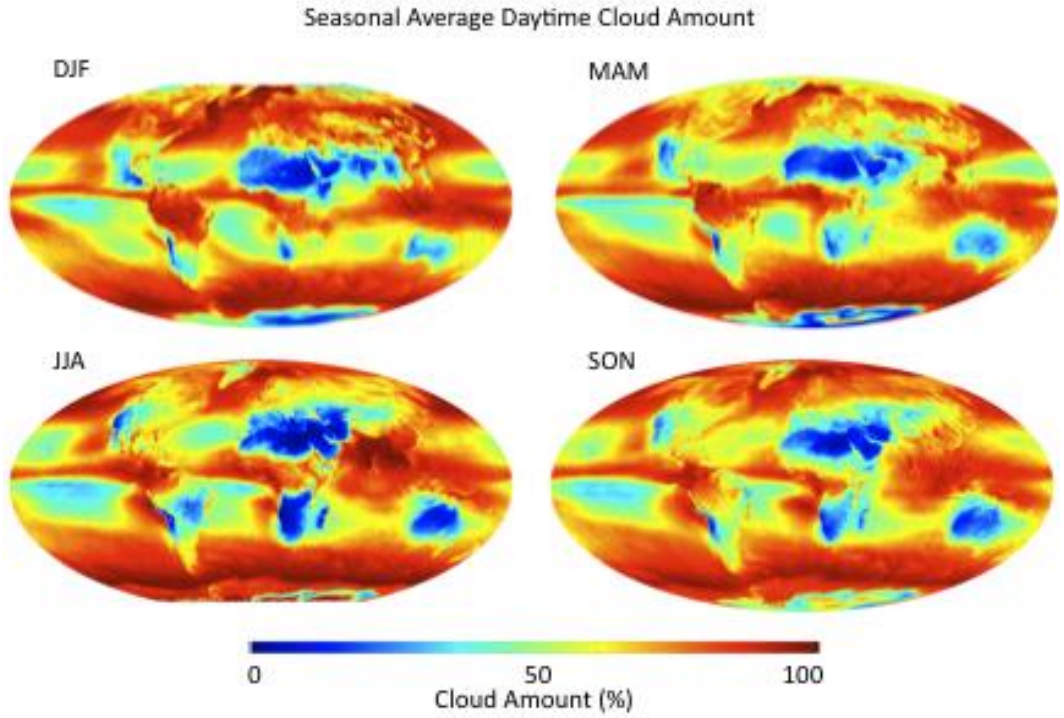

Figure 3. Seasonal mean cloud amount from Terra MODIS shown above is for 2000 through 2009.

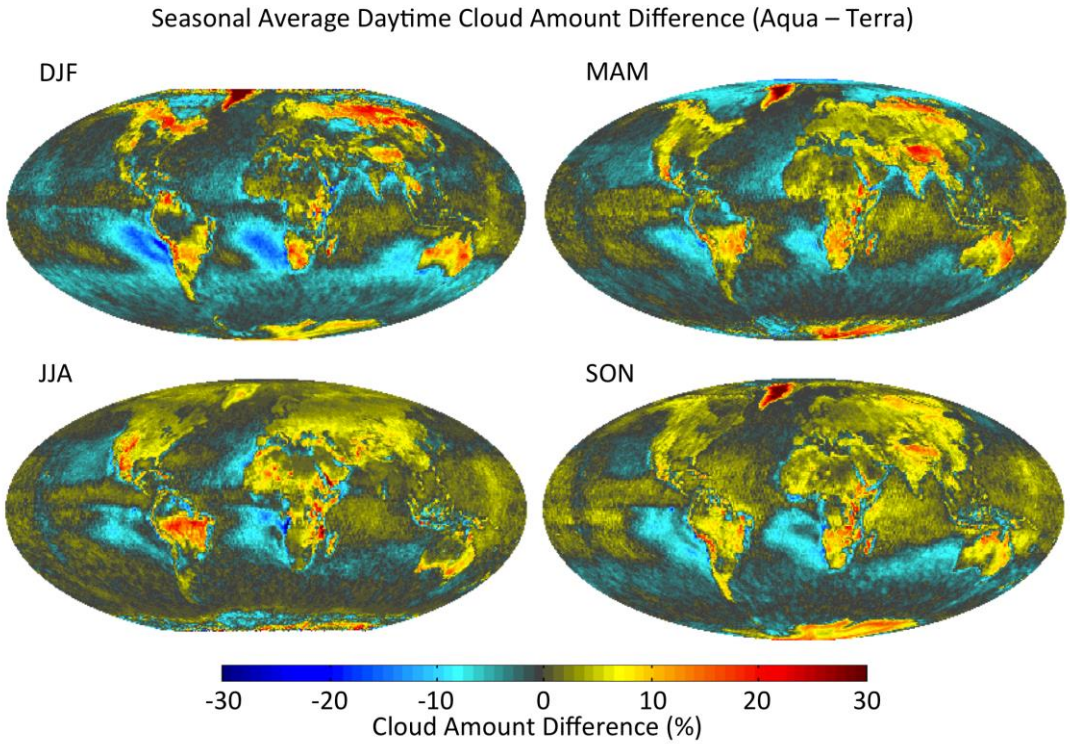

Figure 4. Seasonal mean cloud amount differences between Terra and Aqua MODIS daytime observations.

5.1 Seasonal Cloud Distribution Example

The seasonal means for cloud amount from Terra MODIS capture the seasonal variability of the cloud field (Fig. 3). The seasonal migration of the ITCZ over land and ocean is clearly evident, with the movement of the ITCZ being much more pronounced over land than ocean. The annual cycle of cloudiness in the stratocumulus deck is also evident in the seasonal means, with the annual maximum and minimum extent of the maritime stratocumulus decks being clearly visible between JJA and DJF off the western coastlines of South American and Africa. The influences of the monsoons produce the greatest regional shifts in seasonal cloudiness on the globe. The cloudiness produced over South Asia in JJA by the Indian and South East Asian monsoons is over 90% for JJA and during DJF, the dry season, it is below 30%. There are also small-scale features that are evident in the seasonal cycles. The sea breezes along the tropical coastlines are very pronounced. Also suppression of clouds, relative to the surrounding land, is also clear (e.g. Lake Victoria.)

5.2 Asynoptic Time Sampling

Because Terra satellite operates with a sun-synchronous polar orbit, it samples at two fixed local solar times at each location (i.e., 1030 and 2230 local at the equator) so cannot resolve the diurnal cycle. In contrast, typical model monthly averaged outputs contain the averaged values over a time series of data within a fixed time interval (e.g. every 6 hours). For many constituents in the upper atmosphere, this difference is not likely a problem although for regions influenced

by deep convection and its modulation of the diurnal cycle (e.g. tropical land masses), this time sampling bias should be considered. Fig. 4 shows the differences in the cloud fraction for Aqua-Terra. Differences are generally less than about 30% locally. Globally the difference between Aqua and Terra are ~3%, this relatively smaller difference is due to fewer clouds over ocean and more clouds over land in the afternoon. As a reminder, the CMIP5 cloud amount is the average of day and nighttime orbit observations from the Terra satellite.

5.3 Inhomogeneous Sampling

Because the monthly averaged value in this MODIS data product is an average over observational data available in a given grid cell, the number of samples used for averaging varies with the geo-location of the cell. Because of the convergence of longitude lines near the poles, the time range of data collection broadens as one moves from the equator toward either pole, with the ranges in the polar regions including all times of day and night. So, there are more observations in the regions near the poles (~60° to ~85°) than the rest of the globe. The increased number of overpasses at the poles will occur over a broader portion of the diurnal cycle, this will potentially dampen the amplitude of the observed diurnal cycle in high-latitudes relative to the mid-latitudes and tropics. Therefore, the entire MODIS data set cannot be assumed to be at 1030 local for Terra MODIS.

The day and night algorithms are fundamentally different, the day algorithm contains many tests in the VIS/NIR that are not available at night. These additional tests allow for more cloud types to be detected and better discrimination of clouds and certain surface types (Liu et al 2010). This will lead to seasonal variations in cloud detection capabilities at high latitudes that could be aliased to changes in surface type or atmospheric conditions (e.g. temperature inversions) due to diurnal sampling changes.

6. Instrument Overview

Terra was launched on 18 December 1999, with data available from 24 February 2000, to present. MODIS is a 36-channel whiskbroom scanning radiometer. The channels (referred to as "bands" in the MODIS nomenclature) are distributed between 0.415 and 14.235 μm in four focal plane assemblies, with nadir spatial resolutions of 250 m (two bands), 500 m (five bands), and 1000m (29 bands). The 250 m bands are centered at 0.65 and 0.86 μm with the 500 m bands at 0.47, 0.56, 1.24, 1.63, and 2.13 μm. Each band's spectral response is determined by an interference filter overlying a detector array imaging a 10 km along-track scene for each scan (i.e., 40, 20, and 10 element arrays for the 250, 500, and 1000-m bands, respectively). MODIS has several onboard instruments for in-orbit radiometric and spectral characterization.

MODIS scans a swath width sufficient for providing global coverage every two days from a polar-orbiting, sun-synchronous platform at an altitude of 705 km. Terra is in a descending orbit with an equatorial crossing of 1030 local solar time.

All MODIS atmosphere products are archived into two categories: pixel-level retrievals (referred to as Level–2 products) and global gridded statistics at a latitude and longitude resolution of 1 (Level–3 products). The Level-3 products are temporally aggregated into daily, eight-day, and monthly files containing a comprehensive set of statistics and probability distributions (marginal and joint).

Acknowledgements. Special thanks to the MODIS science and instrument teams.

7. References

Ackerman, S. A., R. A. Frey, K. I. Strabala, Y. Liu, L. Gumley, B. A. Baum, and W. P. Menzel, 2010: Discriminating clear-sky from cloud with MODIS algorithm theoretical basis document (MOD35). MODIS Atmosphere web site, 129 pp.

Ackerman, S. A., K. I. Strabala, W. P. Menzel, R. A. Frey, C. C. Moeller, and L. E. Gumley, 1998: Discriminating clear-sky from clouds with MODIS. *J. Geophys. Res*., 103(D24), 32,141– 32,157.

Ackerman, S. A., R. E. Holz, R. Frey, E. W. Eloranta, B. Maddux, and M. McGill, 2008: Cloud Detection with MODIS: Part II Validation, *J. Atmos. Oceanic Tech.*, 25, 1073-1086.

Bodas-Salcedo, A. et al, 2011: COSP: Satellite simulation software for model assessment. *Bull. Amer. Met. Soc.*, **92**, 1023-1043. doi:10.1175/2011BAMS2856.1

Frey, R. A., S. A. Ackerman, Y. Liu, K. I. Strabala, H. Zhang, J. Key and X. Wang, 2008: Cloud Detection with MODIS, Part I: Recent Improvements in the MODIS Cloud Mask, *J. Atmos. Oceanic Tech.*, 25, 1057-1072.

Holz, R.E., S. A. Ackerman, F.W. Nagle, R. Frey, R.E. Kuehn, S. Dutcher, M. A. Vaughan and B. Baum., 2008: Global MODIS Cloud Detection and Height Evaluation Using CALIOP. *J. Geophys. Res.*, doi:10.1029/2008JD009837.

Hubanks, King, Platnick, and Pincus, 2008: MODIS Atmosphere L3 Gridded Product Algorithm Theoretical Basis Document. *ATBD Reference Number: ATBD-MOD-30. http://modis-atmos.gsfc.nasa.gov/MOD08_D3/atbd.html*

Klein, S. A., Y. Zhang, M. D. Zelinka, R. Pincus, J. Boyle, and P. J. Gleckler, 2012: Are climate model simulations of clouds improving? An evaluation using the ISCCP simulator. Submitted to *J. Geophys. Res.*, in revision (Oct. 2012).

King, M. D., W. P. Menzel, Y. J. Kaufman, D. Tanre´, B. C. Gao, S. Platnick, S. A. Ackerman, L. A. Remer, R. Pincus, and P. A. Hubanks, 2003: Cloud and aerosol properties, precipitable water, and profiles of temperature and humidity from MODIS. *IEEE TGRS*, 41, 442– 458.

Kotarba, A. Z., 2010: Estimation of fractional cloud cover for Moderate Resolution Imaging Spectroradiometer/Terra cloud mask classes with high-resolution over ocean ASTER observations, *J. Geophys. Res*., 115, D22210, doi:10.1029/2009JD013520.

Liu, Y., S. A. Ackerman, B. C. Maddux, J. R. Key, and R. A. Frey, 2010: Errors in Cloud Detection Over the Arctic and Implications for Observing Feedback Mechanisms, *J. Climate*, **23**, 6, 1894-1907.

Pincus, R., S. Platnick, S. A. Ackerman, R. S. Hemler, R. J. P. Hofmann, 2012: Reconciling simulated and observed views of clouds: MODIS, ISCCP, and the limits of instrument simulators. *J. Climate*, doi: 10.1175/JCLI-D-11-00267.1.

Platnick, S., M. D. King, S. A. Ackerman, W. P. Menzel, B. A. Baum, J. C. Rie´di, and R. A. Frey, 2003: The MODIS cloud products: algorithms and examples from Terra. *IEEE TGRS*, 41, 459– 473.

Stubenrauch, C. J., and S. Kinne, 2009: Assessment of global cloud climatologies. GEWEX News, No. 1, International Project Office, Silver Spring, MD 6–7.

Stubenrauch, C. J., W. B. Rossow, S. Kinne, S. Ackerman, G. Cesana, H. Chepfer, B. Getzewich, L. Di Girolamo, A. Guignard, A. Heidinger, B. Maddux, P. Menzel, P. Minnis, C. Pearl, S. Platnick, C. Poulsen, J. Riedi, S. Sun-Mack, A. Walther, D. Winker, S. Zeng, and G. Zhao: Assessment of global cloud datasets from satellites: Project and database initiated by the GEWEX Radiation Panel. *Bull. Am. Meteor. Soc.*, July 2013.

Thomas, S. M., A. K. Heidinger, and M. J. Pavolonis, 2004: Comparison of NOAA's Operational AVHRR-Derived Cloud Amount to Other Satellite-Derived Cloud Climatologies. *J. Climate*, 17, 4805–4822. doi: 10.1175/JCLI-3242.1

8. Useful Links

Relevant MODIS Archive: Level-1 and Atmosphere Archive and Data Distribution System

MODIS Atmosphere Team

MODIS cloud mask product overview and data set description

MODIS monthly cloud fraction browse imagery

MODIS Atmosphere Team publications and references

9. Revision History

Rev 0 – 1/24/2012

Rev 1 – 5/8/2013 (expanded Sect. 5 opening text and additional references)